JOURNAL OF MATERIALS SCIENCE **34** (1999) 2229–2240

Analysis of mold flow and microstructures of die casting in Al alloy/$SiC_{(p)}$ composites

C. B. LIN, C. L. WU, C. H. CHIANG
Department of Mechanical Engineering, Tamkang University, Tamsui, Taipei, Taiwan

The report involves a study of the microstructure of tensile, impact and three-point bending samples of aluminum alloy/$SiC_{(p)}$ composites produced by die casting. The results show that in impact samples, 80 μm SiC particulates cluster along the left and right edges of the section vertical plane with the notch plane, and near the notch. In tensile and three-point bending samples, they were distributed uniformly in the matrix. Furthermore, porosities occurred near the notch in the impact samples. The 80 μm SiC particulates will undergo settling in the shot biscuit. There exist arc and irregular shapes in the clustering section of the particulate. The dendrite arm spacing (DAS) is larger in this section. From the shot biscuit to the bending section of the sprue; the quantity of SiC particulate is less. The SiC particulate is clustered in the protrusive region where the injector pins are situated. We can decrease the porosity of die casting samples effectively by designing the overflow well in a wave shape. We can prevent the melt from adhering to the surface of the mold cavity, thermal cracking on the surface of die casting samples and wear on plungers using electroless nickel plating on the SiC particulate.

1. Introduction

In particulate aluminum matrix composites (PAMC), reinforcement particulates, such as Al_2O_3, SiC, ZrO_2 and Si_3N_4, or lubricative particulates, such as Gr and MoS_2, are distributed uniformly in an aluminum alloy matrix to form materials with special functions and structures. These composites have better specific strength, specific stiffness, hardness and wear resistance than the parent aluminum alloy, and the type and quantity of the second phase can be suitably chosen to adjust the thermal conductivity and coefficient of thermal expansion [1]. They have been used by the aerospace, transportation, electronics and recreation industries for products such as brake rotor discs, electronic packages, printed-circuit board heat sinks, bicycle frames and golf club heads. The development of these composites for industrial use is important [2–5].

In particulate aluminum matrix composites, the distribution of the particulate in the matrix microstructure will affect their properties [6]. Some studies [7, 8] have reported that these composites have low fracture strain, and that the crack initiation and toughness are strongly affected by the distribution and size of the particulate. In particular, these parameters are especially important for the properties when particulate clustering occurs [9, 10]. Lewandowski and Liu [11] reported that cracks initiate in places in the matrix where particulate clustering is observed. Therefore, to understand the fracture behavior of such composites, it is important to observe the particulate distribution in the matrix microstructure.

The phenomenon of non-uniform particulate distribution in the matrix often occurs in PAMC materials [12], and can result from: (1) pushing of the particulates by the aluminum dendrites during solidification [12]; (2) from the Stokes drag force [13]; (3) the van der Waals force of attraction between the particulates before incorporation into the melt [14]; (4) the difference in densities of particulate and melt, the influence of gravity, the cooling rate, etc. [15–17]. Rohatgi *et al*. [14] discussed particle pushing in directionally and rapidly solidified 357/SiC/15p composites, and discovered that the particulate pushing is related primarily to the growth of dendrites. In rapid solidification, because the size of the dendrite arms was smaller, they were not so easily pushed; in unidirectional solidification, the further the distance from the freezing region, the larger the dendrite arm spacing, and the greater the particle pushing. Xie Guohong *et al*. [15] analyzed the composites of Al-4% Mg alloy reinforced with SiC and Al_2O_3 particulates and discovered that for the same kind of particulate, pushing was more difficult with larger particulates; for different kinds of the same size of particulate, SiC particulate was more easily pushed than Al_2O_3 particulate. Stefanescu *et al*. [18] found that the behavior of particulates in the matrix could be divided into three types: (1) pushing, (2) engulfment, and (3) entrapment. At a specific cooling rate, the particulates in densely populated particulate regions are more easily entrapped, while those in less populated regions are more easily pushed. Generally, particulate pushing will lead to particle clustering in the last

TABLE I Chemical composition of (a) the matrix alloy and (b) the die casting Al/$SiC_{(p)}$ composites

(a)

Material system	Si	Fe	Cu	Mn	Mg	Cr	Ni	Zn	Ti	All other elements	Al
A380 (99.7%)	9.75	0.83	3.2	0.41	0.47	—	1.32	—	0.18	0.2max	rem.
A360 (99.7%)	9.63	0.68	0.1	0.05	0.57	—	—	0.05	—	0.2max	rem.

(b)

Composites materials	DI	DII	DIII
Matrix	A360	A360	A380
Strengthen phase	80 μm SiC	80 μm SiC*	80 μm SiC +15 μm SiC
Weight per cent	10	10	10 + 5

*: With electroless plating nickel in the surface of the SiC particulate.

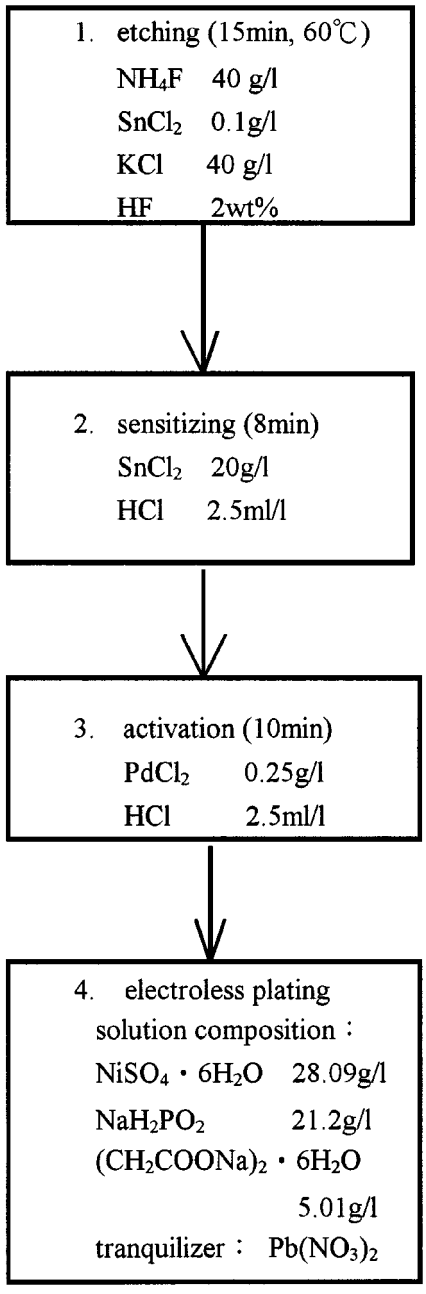

Figure 1 Schematic diagram showing the process of electroless plating of the SiC particulates with nickel.

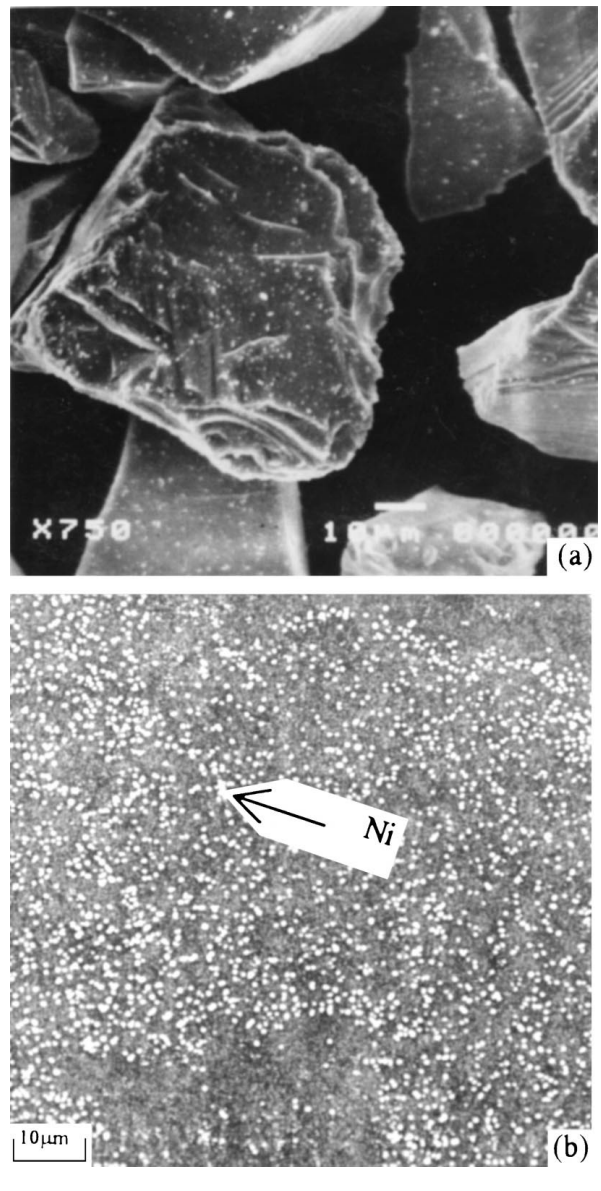

Figure 2 (a) SEM micrographs and (b) mapping on SiC particulate after electroless plating with nickel.

solidification regions [19], and their distribution will depend upon the interactive force between the particulates and the behavior of the moving solidification front [20]. To quantitatively compare the pushing and

TABLE II The parameters of die casting

Die casting machine	350 tons	Velocity of gate	42.15 $m\,s^{-1}$
No. of cavities	3	Diameter of plunger	57.15 mm
Mold temperature	$200 \pm 3\,^{\circ}C$	Velocity of plunger	2.6 $m\,s^{-1}$
Thickness of gate	1.7 mm	Filler time	0.056 s
		Al alloy melting temperature	$680 \pm 5\,^{\circ}C$

Three cavities for tensile, impact, and three-point bending test samples.

distribution of particulates, Xie Guohong *et al*. [15] indicated that the effects of the particle type and size of SiC, Al_2O_3, or SiO_2 particle reinforced Al-4% Mg composites on the pushing behavior during solidification, and the intensity of pushing during the solidification was determined by the mass ratio of equiaxed cell to particle.

AMC products have been made using traditional manufacturing methods, such as casting, forging, extrusion, etc. When using gravity casting for near net-shape products, porosities are often produced if the flow gating system has not been suitably designed. In comparison, with die casting, castings may be produced at a faster rate and lower cost, with less porosity. In addition, if better die castings are required, a steady metal flow into the die cavity is required. As the air in the cavity can produce porosity when surrounded by the melt and reduce the mechanical properties of the castings, it is important to maintain turbulence when pouring to a minimum, although a certain amount is inevitable. Therefore, to maintain the quality of a casting in the die casting process, the design of the flow system obviously plays an important role. As very few studies covering particulate aluminum matrix composites using die casting processing have been reported [21, 22], the present work was undertaken to investigate the production of $A360/SiC_{(p)}$ and $A380/SiC_{(p)}$ aluminum matrix composites, using the die casting process, and a flow system designed by the authors. As the mechanical properties of composites are their main point of interest, the die casting produced was designed such that tensile, impact and three-point bending samples could be sectioned from the casting for testing purposes. As the mechanical properties of the composite are strongly influenced by the size and distribution of the particulate, the SiC particulate distribution in the flow system was studied in particular, as well as the effects of particulate size and nickel coating on the former. So we

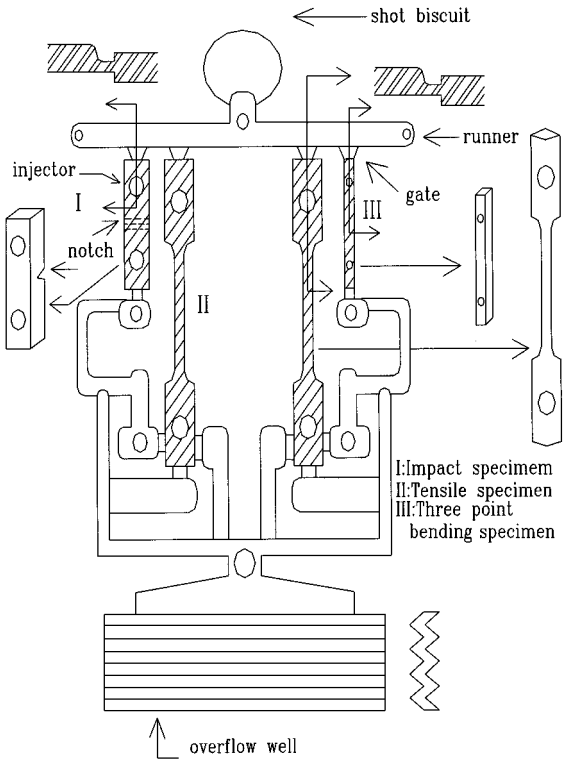

Figure 3 Schematic diagram of the die casting mold showing the flow system design.

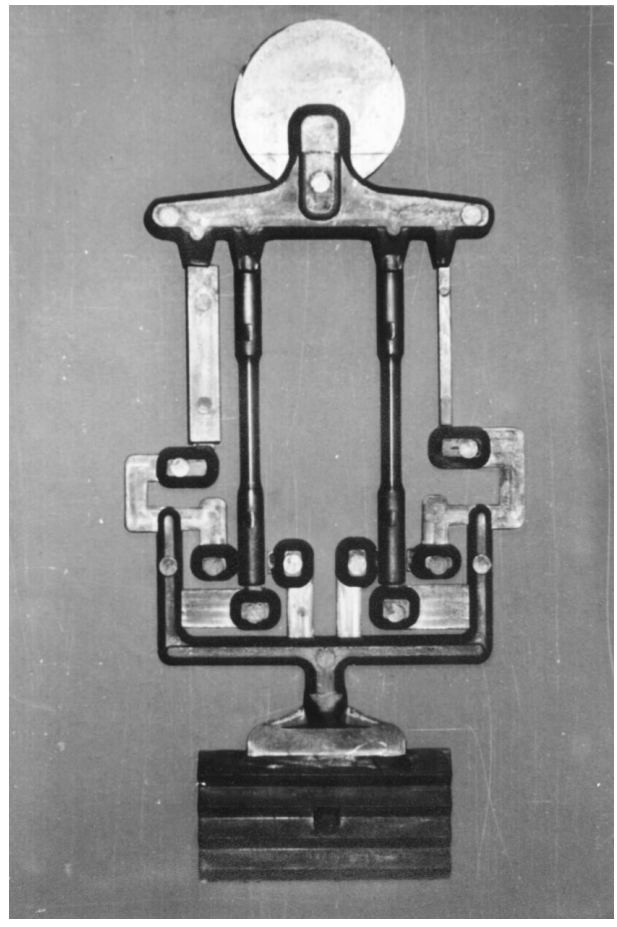

Figure 4 Tensile, impact and three-point bending test samples made by die casting.

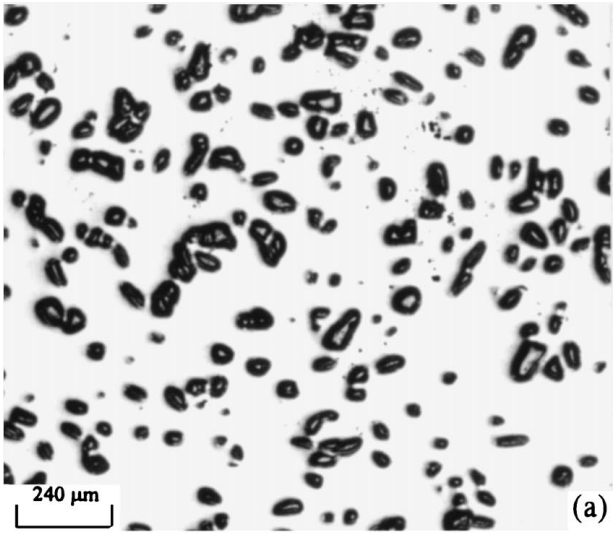

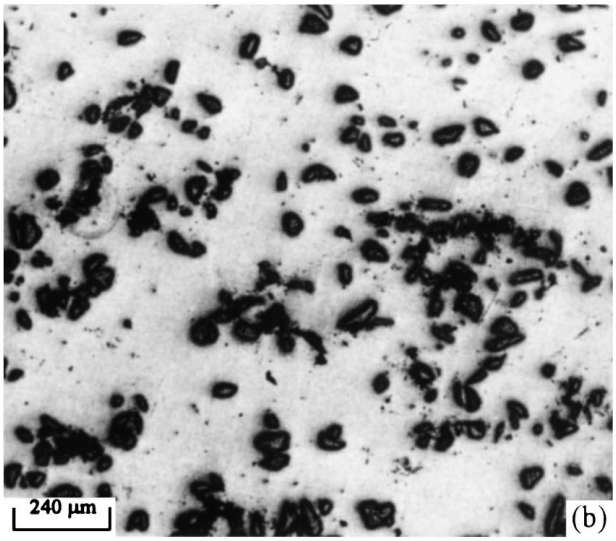

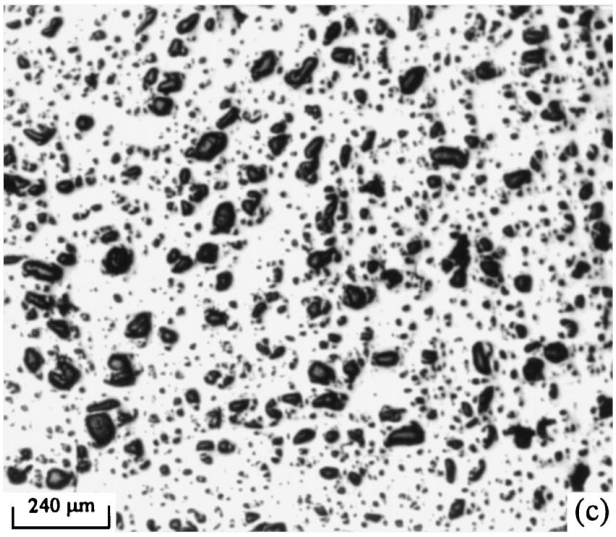

Figure 5 Optical micrographs showing SiC particulate distribution in (a) DI, (b) DII and (c) DIII matrix alloys.

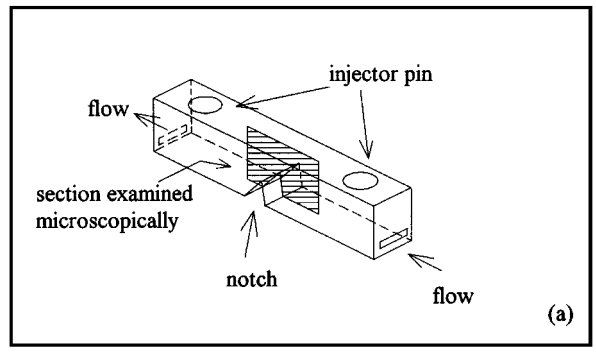

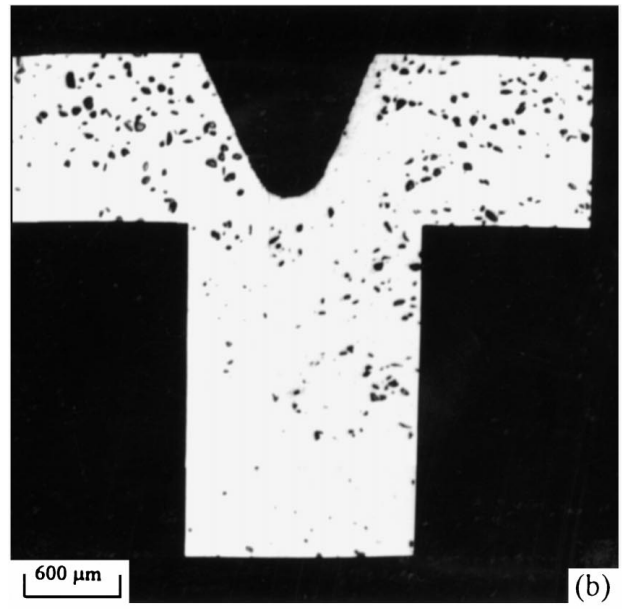

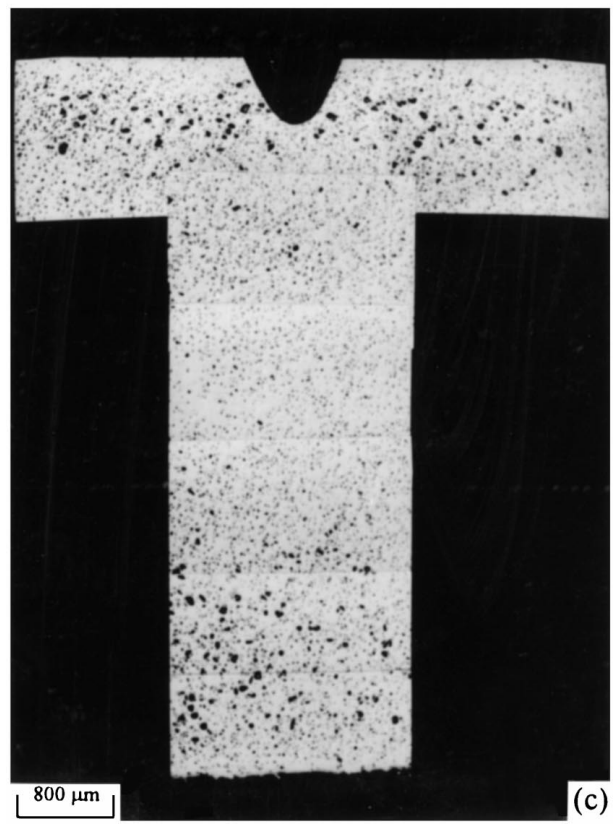

Figure 6 (a) Schematic diagram showing the section of impact sample examined optically, perpendicular to the notch plane; (b), (c) optical micrographs showing SiC particulate distribution in (b) DI and (c) DII composite matrices.

will use the above-mentioned flow system and cast with A360/$SiC_{(p)}$ and A380/$SiC_{(p)}$ aluminum matrix composites using die casting, and discuss the distribution of SiC particulate in the flow system observed with an optical microscope (OM). Meanwhile, we will discuss how the size and the surface electroless plated nickel

of particulate effect the distribution of particulate in matrix.

The aim of this study is to provide a reference for the die casting of AMC materials.

2. Experimental procedure

The materials used in the present study are A360/10 wt % $SiC_{(p)}$ composites [DI], A360/10 wt % $SiC^{*}_{(p)}$ composites [DII], and A380/10 wt % $SiC_{(p)}$ + 5 wt % $SiC^{**}_{(p)}$ composites [DIII]. The average compositions of the A360 alloy (purity 99.7%) and A380 alloy (purity 99.7%) used in present study are shown in Table I, where the average size of the $SiC_{(p)}$, $SiC^{*}_{(p)}$ and $SiC^{**}_{(p)}$ are 80 μm, 80 μm and 15 μm, β phase, irregular shape, purity (99.9%), SiC^{*} with electroless plating nickel in the surface of SiC particulate. The purpose of electroless plating nickel is to improve the wetting ability of the interface between SiC particulates and Al alloy matrix, and promote the joining properties of the interface. The process of electroless plating with nickel is shown in Fig. 1. Fig. 2a shows a scanning electron micrograph of nickel-plated SiC particulates. From the corresponding Ni X-ray image (Fig. 2b), we know that the surface of the SiC particulate has been uniformly plated with nickel. We have used this technology [23] to prepare A360/$SiC_{(p)}$ and A380/$SiC_{(p)}$ aluminum matrix composites.

Using a melt of composites at 700 °C, in all cases, the melt was stirred continuously, using a specially designed impeller made of graphite. The stirring was such that no whirlpools formed, and the SiC particulate was well mixed within the melt, to assure the SiC particulate was incorporated in the alloy.

As mechanical property testing of die castings is generally carried out, in the present study, the die casting mold used was designed to provide tensile, impact and three-point bending specimens. A schematic diagram of the die casting mold and the flow system design is shown in Fig. 3, while the die casting parameters are given in Table II. The mold was fabricated from SKD 61 material then subjected to carbonitriding to enhance the mold hardness to HRC 60.

During the entire process of the die casting, it was necessary to prevent the SiC particulate from sinking to the bottom of the melt as a result of gravity. Stirring with a graphite agitator and impeller continuously is required in the melt of composites, as well as averting whirlpools in the course of agitation. Owing to the fact that different mold temperatures will directly affect the properties of die casting, the temperature of the mold must be equal to the thermal equivalent after die casting several times. We can therefore obtain the die casting samples required, and to ensure the properties of die casting reach the steady state.

Several sections were cut from the die cast samples. After mounting, the samples were polished using SiC abrasive paper (from #200 to #1200 grade), followed by polishing with a liquid suspension of 0.3 μm Al_2O_3 particulates in water. The polished samples were then examined for SiC particulate distribution, using a Nikon optical microscope.

3. Results and discussion

3.1. Distribution of SiC particulates in the die casting

The tensile, impact and three-point bending test samples made by die casting are shown in Fig. 4. The distribution of SiC particulate in the matrix is uniform, shown in Fig. 5a to c except for the sample from the impact test including 80 μm SiC particulates that are clustering in the left and right edges of the section vertical with notch plane and near notch. The cross-section of the impact sample was examined optically, vertical with the notch plane is shown in Fig. 6a, and the distribution of SiC particulate in DI and DIII composite matrices are shown in Fig. 6b and c, respectively. From the micrographs, we can see that the 80 μm SiC particulates cluster in the left and right edges of the section vertical with the notch plane and along the notch tip ($\pm 45^{\circ}$), Fig. 6a. In the DIII composite, the 80 μm SiC particulates are distributed in the edges, but the 13 μm SiC particulates are distributed uniformly throughout the matrix, as shown in Fig. 6c. During the die casting process, the molten metal flows into the cavity, and the cavity is filled from bottom to top. A schematic diagram of the flow is shown in Fig. 7. Filling takes place as follows: the molten metal flows into the cavity from the gate, in fountain-like fashion, with some of the metal in the corner flowing along the wall of the cavity affected by gravity, as shown in Fig. 7a and b. When the filling is near the notch, turbulence will occur, as shown in Fig. 7c. When filling is continuous, the molten metal in the top left part in Fig. 7c will fall along the notch plane, so there will be circulation of the molten metal and, hence,

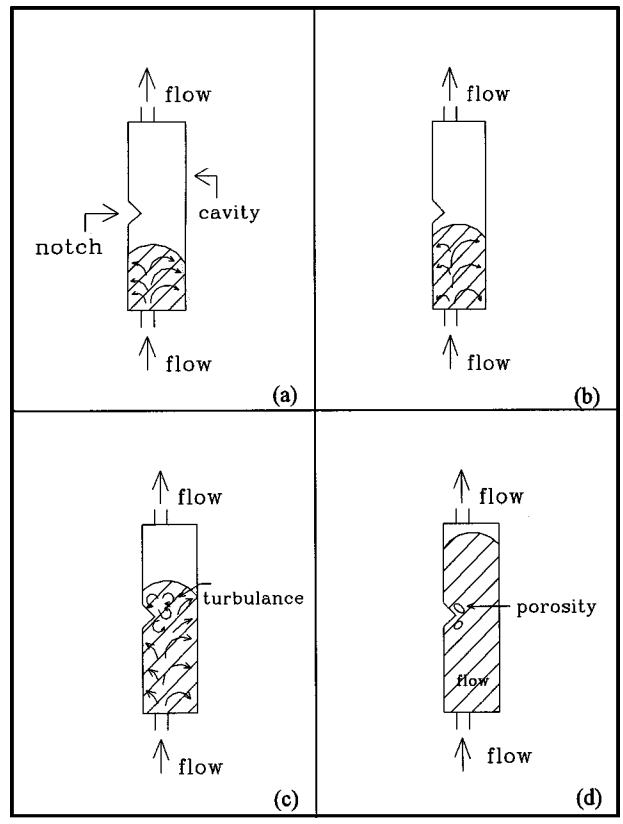

Figure 7 Schematic diagram showing melt flow during the die casting process.

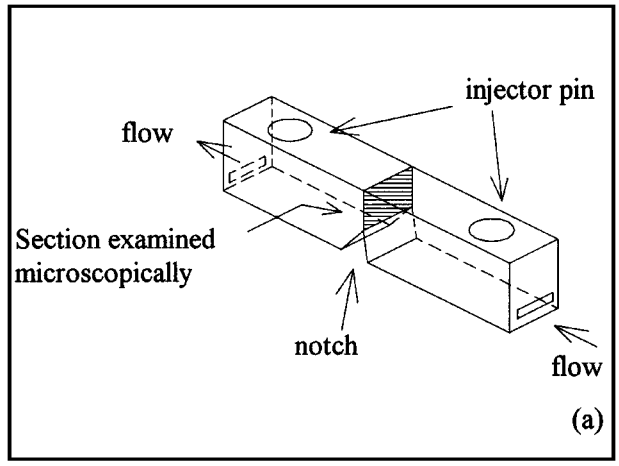

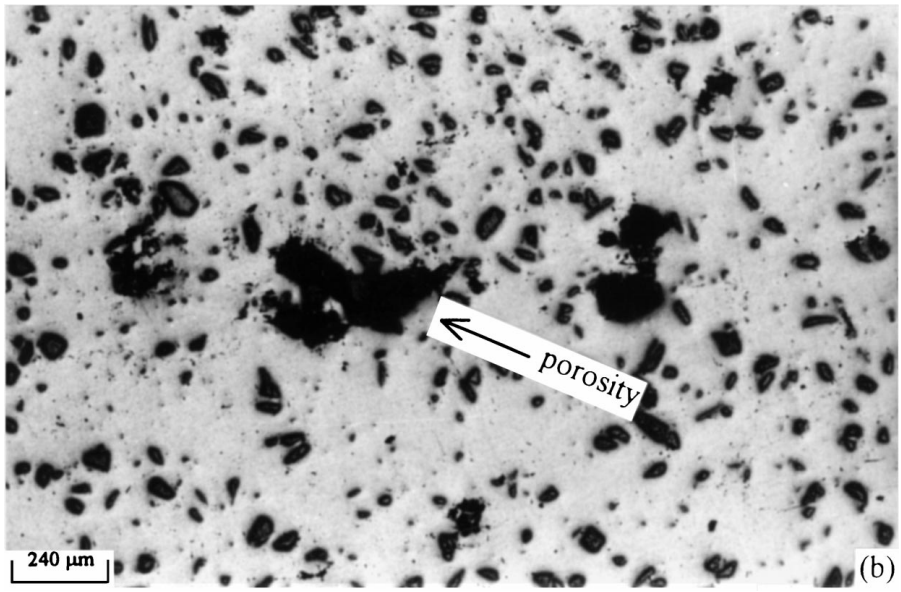

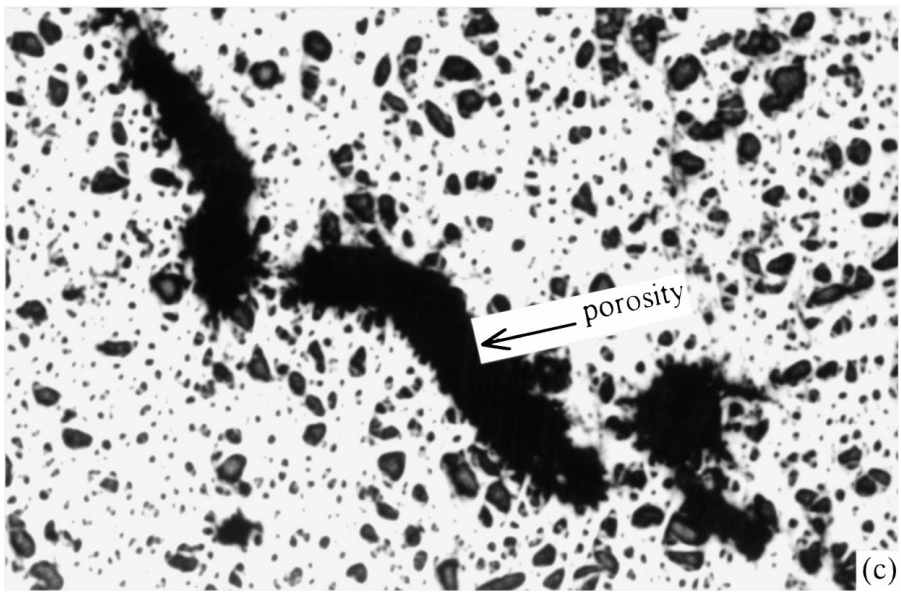

Figure 8 (a) Schematic diagram showing the section of impact sample examined optically, parallel to the notch plane; (b), (c) optical micrographs showing the SiC particulate distribution and porosities in (b) DI and (c) DII composites.

turbulence occurring near the notch plane. The 80 μm SiC particulates ($\rho = 3.12$ g cm^{-3}) being heavier than the liquid metal ($\rho = 2.78$ g cm^{-3}), are easily scattered to the edges of the cavity. Because the filling time is short, these SiC particulates will be entrapped immediately by the solidifying matrix near the wall of the cavity, and we can see the 80 μm SiC particulates clustering more in both left and right edges of the vertical

sections shown in Fig. 6b and c, than in other regions. In comparison, the 13 μm SiC particulates are lighter than the 80 μm SiC particulates, so the phenomenon of clustering is not that obvious. Also, because of the circulation and turbulence, the 80 μm SiC particulates will be distributed near the notch, and we can find here have easily air is involved in forming porosities at the tip of the notch plane as shown in Fig. 7d, and is not so easy to exclude, as seen in the optical micrographs of Fig. 8.

Thus, in the case of composite die castings, when we design the flow system of the die casting, if the casting has non-continuous shapes (such as a notch) or if a larger size of particulate is used, particulate clustering in the matrix and the formation of porosities will also have to be considered.

3.2. Distribution of SiC particulates in the shot biscuit

Fig. 9a shows the region of the shot biscuit that was optically examined. The micrograph in Fig. 9b shows the SiC particulate distribution, where segregation of the 80 μm SiC particulate is observed, whereas the 13 μm SiC particulate distribution over the shot biscuit is uniform. The clustering of the 80 μm SiC particulate is explained on the basis of the fact that (i) the shot biscuit region is the last to solidify, and (ii) the density of the SiC particulates is greater than the aluminum alloy melt, so they tend to settle to the bottom. Although the SiC particulates are uniformly distributed in the die casting, such settling in the shot biscuit will lower the quantity of SiC in other sections.

Thus, one needs to pay attention to the problem of settling; especially if the particulate size is larger or the density is much higher compared to the aluminum alloy melt. Owing to the phenomenon of turbulence in the whole shot biscuit die casting flow, the SiC particulates clusters randomly in a region, making the SiC particulate cluster in the irregular shape of an arc as shown in Fig. 10a and b, respectively. In addition, we can find the dendrite arm spacing (DAS) of SiC particulate clustering regions is greater, whereas, the DAS regions without particulate is smaller, as shown in Fig. 10c. In addition, an obvious demarcation line exists between the region of DAS sizes. This is because in the region with more particulate clustering, the specific heat will increase relatively. So the particulate clusters, makes the cooling rate here lower than in the region that has no particulates. This shows the rate of solidification and there is enough time for the dendrite to grow. In general, the thickness of the shot biscuit is usually about 3–15 mm. In the present study, the thickness of the shot biscuit was varied from 11 mm to 47 mm, to determine its effect on segregation of the particulates.

3.3. Distribution of SiC particulates in the vertical runner

The runner is the passage that connects the shot biscuit and gate, to allow the liquid melt to flow into the

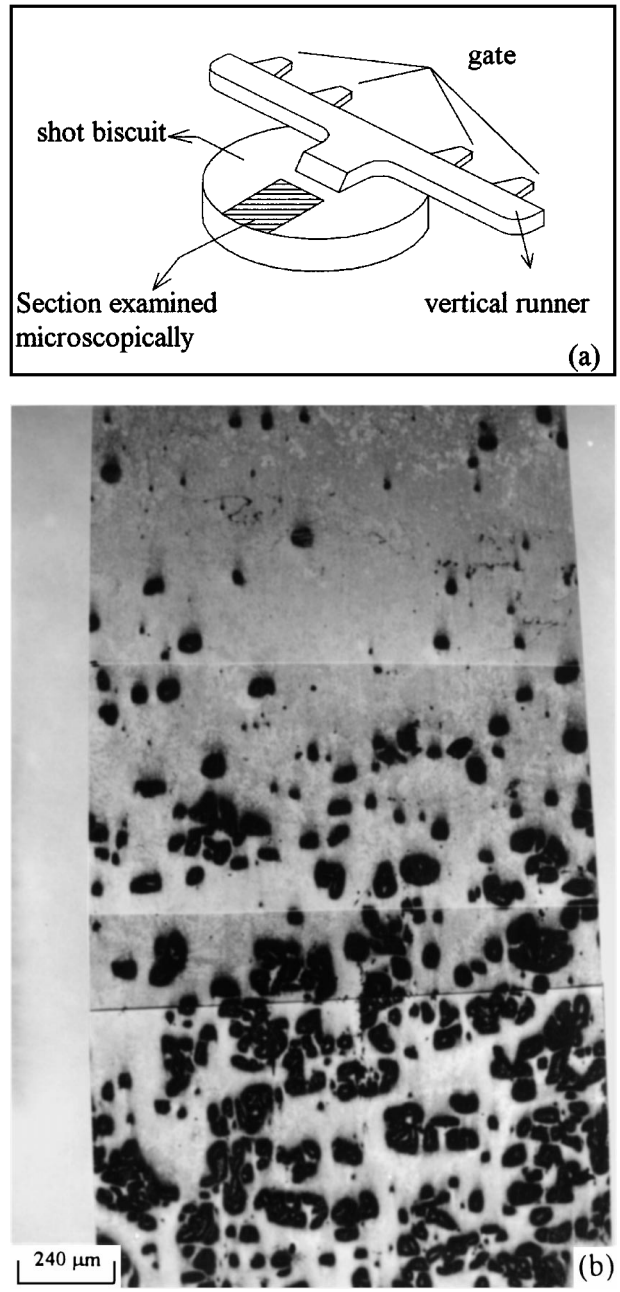

Figure 9 (a) Schematic diagram showing the section of shot biscuit examined optically and (b) optical micrograph showing SiC particulate distribution in shot biscuit.

cavity efficiently. The region of the vertical runner observed microscopically is shown in Fig. 11a, the melt flow from shot biscuit to vertical runner is shown in Fig. 11b and the distribution of the SiC particulate in matrix between shot biscuit and vertical runner is shown in Fig. 11c. From the photograph we can see the dendrite arm spacing (DAS) in the matrix of the shot biscuit is larger, but the DAS in the vertical runner is smaller. The reason is that the melt in shot biscuit solidified more slowly than in the vertical runner, so the dendrite arm had enough time to grow. The amount of particulate in the shot biscuit is larger than in the vertical runner. If we observe all the distributions of SiC particulate in the shot biscuit and vertical runner, we find less particulate in the curved region of the vertical runner as shown in Fig. 11c, and in the other regions, the particulate is distributed uniformly. So, distribution of SiC particulates in Fig. 11c is in two obvious regions, caused by melt

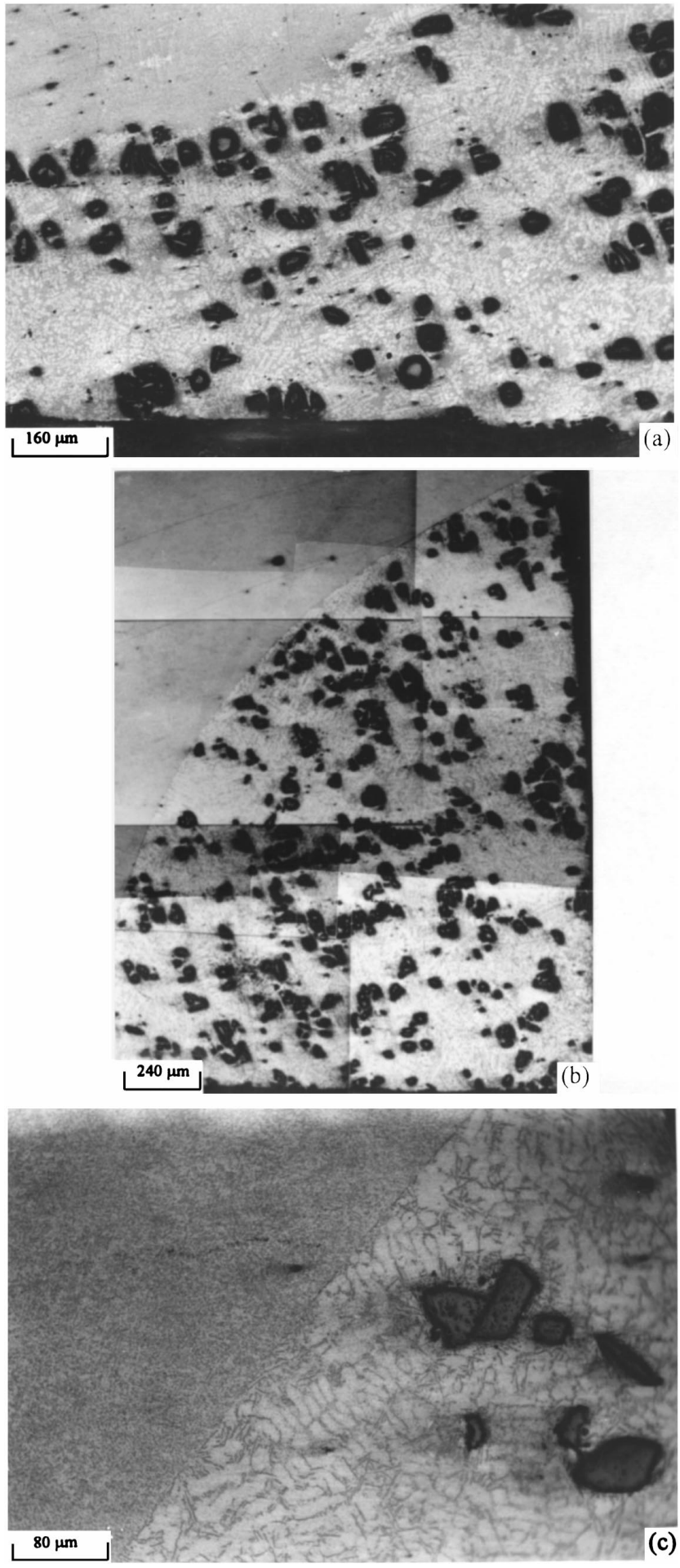

Figure 10 Optical photomicrograph of SiC particulate cluster distributed in the matrix and the cluster region formed the shape of (a) arc and (b) irregular; (c) the dendrite arm of SiC particulate clustering region and without particulate region.

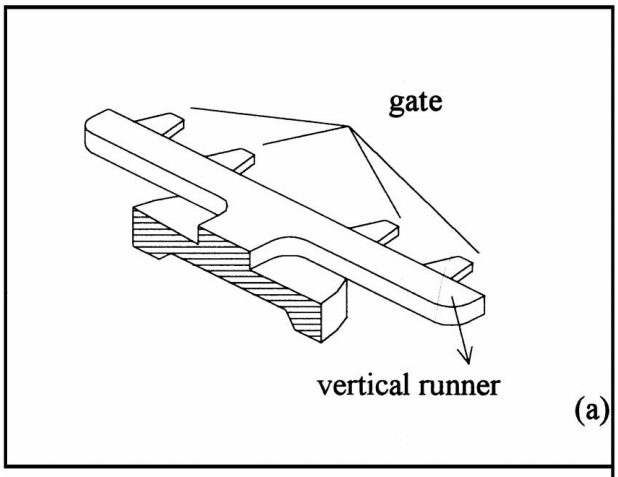

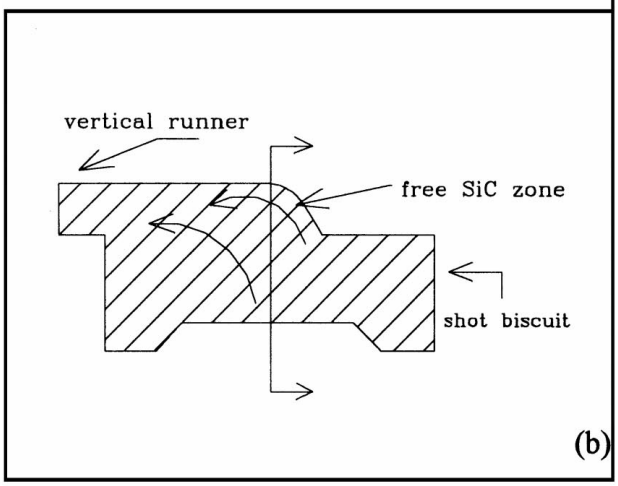

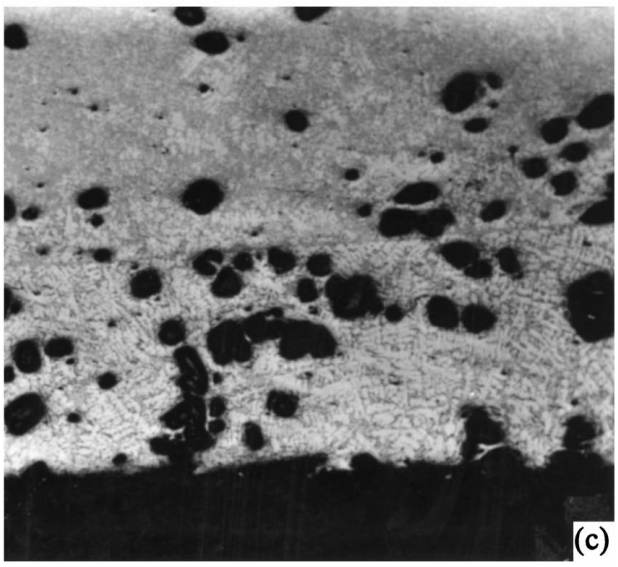

Figure 11 (a) Observational region of optical microscope of vertical runner, (b) schematic diagram of the melt flow from shot biscuit to vertical runner and (c) optical micrograph of SiC particulate distributed in the matrix between shot biscuit and vertical runner.

flowing through the vertical runner of a 70° curve runner. The melt involves the air easily when it is flowing around the corner, and that place will generate a low pressure region for the initial period, and in the later period, the melt will flow into the low pressure region through permeation. We can thus see that there is less SiC particulate near the corner. To prevent the formation of porosities, low pressure regions or whirlpools, the shape of the gate should not change sharply in design.

3.4. Effect on the design of injector pins

The purpose of setting up injector pins is to push die castings out of molds. In general design, the mold extends several millimeters above the free surface where the injector pins were situated Fig. 12a shows the protrusive region of injector pins observed by optical microscopy. From Fig. 12b and c we can find that SiC particulate cluster on the protrusive region in DI and DII, but less particulate is seen around the injectors. 80 μm SiC particulate clusters more on the protrusive region in DIII, but 13 μm SiC particulate is distributed uniformly in the matrix. When polishing the protrusive region down to the free surface of the sample, SiC particulate clusters in the region disappears, as shown in Fig. 12e. If polishing continues to remove the last vestige of injectors, all the SiC particulate is distributed well on the matrix as shown in Fig. 5. The above result is because the melt of composites in the process of filling diverges, 80 μm SiC particulates tend to cluster on two sides and the injector pins create a protrusive region, so SiC particulates tend to cluster here easily allowing this region to collect more particulate. Also, in the free surface of the die casting sample a thin layer exists without SiC particulate. When this surface is polished more particulate appears here, and less in the other regions. If we keep polishing out the thin layer of free surface in the die castings, SiC particulate appears in the internal parts.

3.5. Effect on the design of overflow wells

The purpose of an overflow well is, when filling, the air and some impurities in the cavity can be taken into this overflow well, preventing the formation of porosities, improving the flow of melt and adjusting the local temperature of the cavity. There are two designs of overflow wells in the present study shown in Fig. 13a and b. One is a wave-shaped overflow well (type I) and the other is a fan-shaped overflow well (type II) and their microstructures seen under an optical microscope are as shown in Fig. 13c and d. From this photograph we know there is less porosity in type I than in type II, resulting from the air in the cavity having been pushed into the wave-shaped overflow well in the initial period of filling and the flow field of the die casting is further; for type II, the flow field of the die casting is shorter and easily produces back pressure, so the air in the cavity is not easily excluded. If type I and type II die castings are placed into an air furnace at 500 °C, and after 2 h put into water to quench, the type II die casting has blisters in its surface. This shows that type II design die casting is not ideal and wastes materials. The recycling of particulate metal matrix composites is difficult and the cost is high. So, to reduce the cost of die casting using these materials, the wave-shape overflow well is suggested.

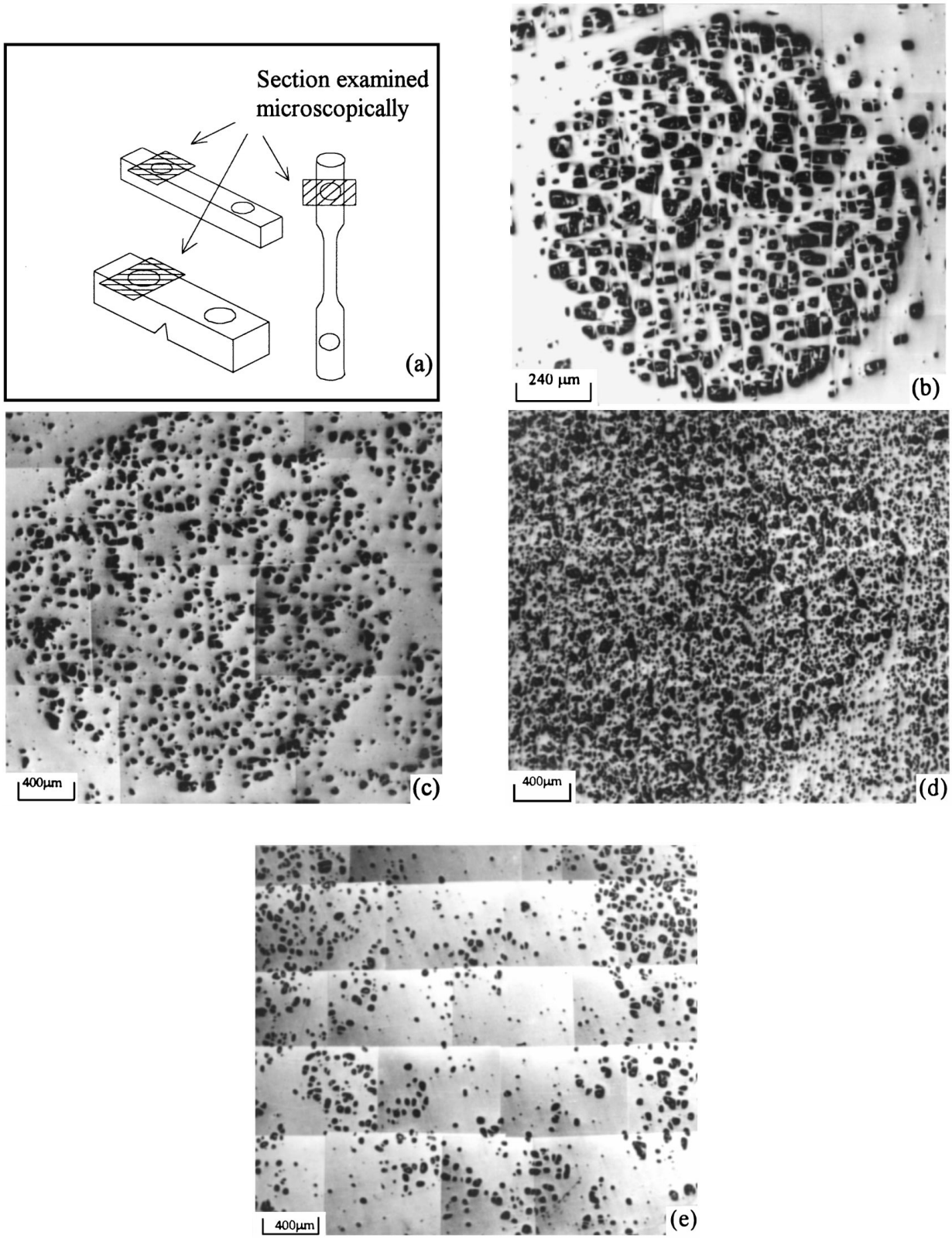

Figure 12 (a) Observed region of injector pins by optical microscope; optical micrograph of SiC particulate distributed in injector pin in (b) DI, (c) DII, (d) DIII and (e) after polishing the surface on the protrusive region to the free surface of DII sample.

3.6. Influence of SiC particulate electroless plating with nickel

SiC particulate has unstable thermodynamics at high temperatures, so it easily produces the reaction $4Al_{(1)} + 3SiC_{(s)} \rightarrow Al_4C_{3(s)} + 3Si_{(1)}$ with melted aluminum alloy at the interface, and forms brittle intermetalic compounds such as Al_4C_3 [24]. Simultaneously, the viscosity of the composites will have increased and the quantity of Al_4C_3 will have also increased with time. In industry, the process time of die casting is long, so the viscosity of the melt will be increased with time and will affect the flow of die casting and reduce the mechanical properties of the products. To avoid the viscosity increasing with time, electroless nickel plating can be used on the surface of SiC particulate uniformly to reduce the interface product and

promote the joining property of the interface. From experiment it is clear that SiC particulate with electroless nickel plating is necessary for the long-time process of die casting. So, SiC particulate plates without nickel, will give rise to certain negative effects after long time die casting. These are: (1) The die casting adheres easily to the surface of the mold cavity; (2) Because of the increment of viscosity, the pressure must be high, although this could result in the wearing of the head of the plunger; (3) Thermal cracking results easily on the surface of die castings. If the SiC particulates are nickel plated, these defects will not occur and we can also see the distribution of SiC particulate plating nickel in the matrix is similar to that in the DI system.

4. Conclusions

Tensile, impact and three-point bending die cast samples of A360/10 wt % $SiC_{(p)}$, A360/10 wt % $SiC^{*}_{(p)}$ and A380/10 wt % $SiC_{(p)} + 5$ wt % $SiC^{**}_{(p)}$ aluminum matrix composites were successfully manufactured in the present work, and the effects of the flow system design, size of particulate, and electroless plating of the SiC particulates with nickel was also studied. With reference to the die casting of SiC particulate aluminum matrix composites, the following may be concluded:

(1) Except for the sample of impact 80 μm SiC particulate that clustered in the left and right edges of the section vertical with the notch plane and the site of the notch tip, 13 μm SiC particulate and 80 μm SiC particulate distributed uniformly in the matrix in all die casting samples.

(2) There are porosities near the notch tip in the impact sample.

(3) 80 μm SiC particulate segregates in shot biscuit; yet the distribution of 13 μm SiC particulate is very uniform in the matrix.

(4) Increasing the thickness of the shot biscuit results in SiC particulate clustering in the arc and irregular regions. The size of DAS in the shot biscuit is larger where there is SiC particulate cluster, and there is an obvious demarcation line between the larger DAS and smaller DAS.

(5) From shot biscuit to the 70° arc of the vertical runner turbulence in the region reduces the quantity of SiC particulate.

(6) On the surface of the protrusive region, SiC particulate clustering occurs; on the sub-surface, we discovered this area has a lower quantity of SiC particulate but in the vicinity of the region, the SiC particulate is distributed uniformly. Further into the internal parts, SiC particulate is distributed uniformly in the matrix.

(7) An overflow well designed in the shape of waves can help reduce the porosity in the die casting.

(8) Electroless nickel plating of the SiC particulate surface can assist in maintaining the die casting process parameters, as factors such as adherence to the mold cavity surface, thermal cracking on the surface of the die cast sample, and wearing of the plunger are minimized. In addition, the nickel plating is not found to influence the particulate distribution.

Acknowledgements

This work has been supported by the National Science Council, Taiwan. We also would like to thank Mr M. G. Shau for preparing the die-cast samples.

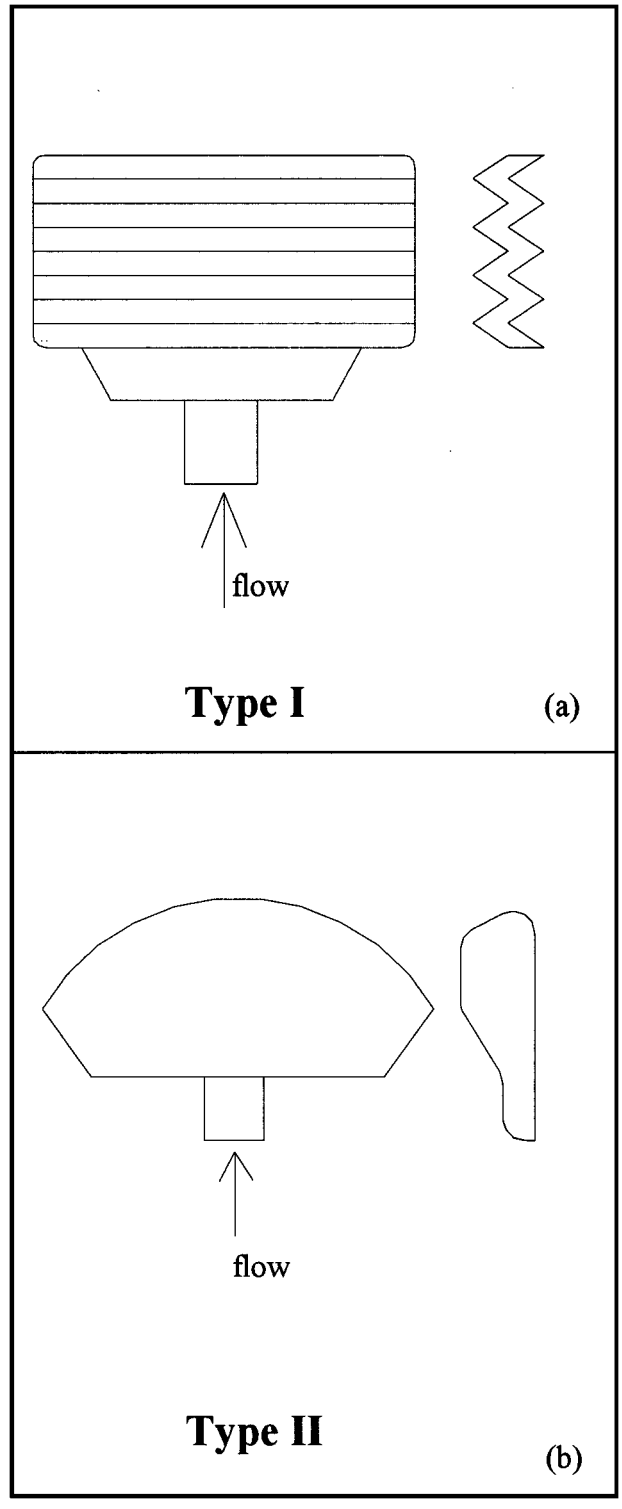

Figure 13 Schematic diagrams of overflow well (a) type I: wave shape and (b) type II: bulk shape; optical micrographs of (c) type I and (d) type II of overflow.

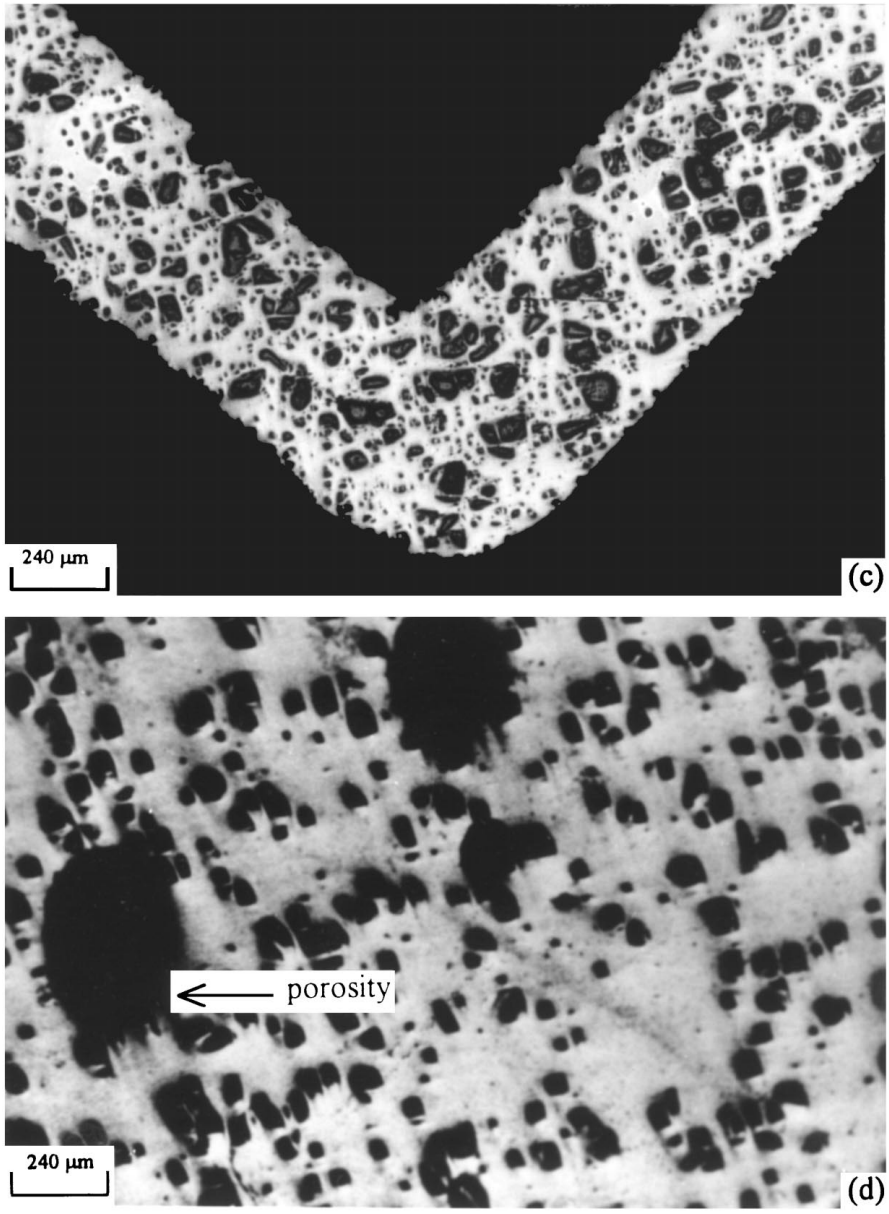

Figure 13 (Continued).

References

1. D. F. HASSON, S. M. HOOVER and C. R. CROWE, *J. Mater. Sci.* **20** (1985) 4147.
2. D. E. HAMMOND, *Modern Casting*, Aug. (1989) 29.
3. D. M. SCHUSTER, M. D. SKIBO and W. R. HOOVER, *Light Metal Age*, Feb. (1989) 15.
4. K. MARSDEN, *J. Met.* **37** (1991) 37.
5. K. S. RAVICHANDRAN and E. S. DWARAK, *ibid.* **39** (1989) 28.
6. W. A. LOGSDON and P. K. LIAW, *Eng. Fract. Mech.* **24** (1986) 737.
7. D. L. MCDANELS, *Metall. Trans. A* **16** (1985) 105.
8. T. CHRISTMAN, A. NEEDLEMAN, S. NUTL and S. SURESH, *Mater. Sci. Eng. A* **107** (1989) 49.
9. J. D. EMBURY, *Metall. Trans. A* **16** (1985) 219.
10. J. R. FISHER and J. GURLAND, *Metall. Sci.* **15** (1981) 185.
11. J. J. LEWANDOWSKI and C. LIU, *Mater. Sci. Eng. A* **107** (1989) 241.
12. A. M. SAMUEL, A. GOTMARE and F. H. SAMUEL, *Compos. Sci. Technol.* **53** (1995) 301.
13. D. SHANGGUAN, S. AHUJA and D. M. STEFANESCU, *Metall. Trans. A* **23** (1992) 669.
14. P. K. ROHATGI, F. M. YARANDI, Y. LIU and R. ASTHANA, *Mater. Sci. Eng. A* **147** (1991) L1.
15. G. XIE, S. LI, W. WANG and R. WU, *Acta Metall. Mater.* **31** (1995) B275.
16. D. J. LLOYD, *Compos. Sci. Technol.* **35** (1989) 159.
17. S. GOWRI and F. H. SAMUEL, *Metall. Trans. A* **23** (1992) 3369.
18. D. M. STEFANESCU, B. K. DHINDAW, S. A. KACAR and A. MOITRA, *ibid.* **19** (1988) 2847.
19. D. M. STEFANESCU, D. SHANGGUAN and P. BRINCKEN, *Mater. Sci. Forum* **77** (1991) 25.
20. P. K. ROHATGI, R. ASTHANA and S. DAS, *Int. Met. Rev.* **31** (1986) 115.
21. M. R. GHOMASHCHI, *J. Mater. Process Technol.* **52** (1995) 193.
22. S. SULAIMAN and T. C. KEEN, *ibid.* **65** (1997).
23. C. B. LIN, US Patent 540 338, March (1995).
24. N. HAN, G. POLLARD and R. STEVENS, *Mater. Sci. Technol.* **8** (1992) 184.

Received 7 October 1997
and accepted 20 August 1998